



Taxonomic reassessment of *Pseudohaptolina birgeri* comb. nov. (Haptophyta)

CATHERINE GÉRIKAS RIBEIRO ^{1,2}, ADRIANA LOPES DOS SANTOS ³, IAN PROBERT ⁴, DANIEL VAULOT ^{1,3}, AND BENTE EDVARDSEN ⁵

¹Sorbonne Université, CNRS, UMR7144, Team ECOMAP, Station Biologique, Roscoff, 29680, France

²GEMA Center for Genomics, Ecology & Environment, Universidad Mayor, Camino La Pirámide, 5750, Huechuraba, Santiago 8580745, Chile

³Asian School of the Environment, Nanyang Technological University, 50 Nanyang Avenue, Singapore 639798, Singapore

⁴Roscoff Culture Collection, Sorbonne Université, CNRS, FR2424, Station Biologique, Roscoff, 29680, France

⁵Department of Biosciences, Section for Aquatic Biology and Toxicology, University of Oslo, P.O. Box 1066 Blindern, Oslo NO-0316, Norway

ABSTRACT

The haptophyte genus *Pseudohaptolina* (formerly *Chrysochromulina* clade B1-3) currently harbours two species: *Pseudohaptolina arctica* and *Pseudohaptolina sorokinii*. In addition, *Chrysochromulina birgeri* is expected to belong to this genus due to its morphological similarity to *P. sorokinii*, but it has not yet been genetically characterised. A strain belonging to *Pseudohaptolina* was brought into culture from Arctic waters, characterised by 18S and 28S rRNA gene sequencing as well as optical and transmission electron microscopy, and deposited in the Roscoff Culture Collection with the code RCC5270. Molecular and morphological data from RCC5270 were compared with those from previously described *Pseudohaptolina* and *Pseudohaptolina*-like species. Strain RCC5270 showed strong phylogenetic affinity to *P. sorokinii*, but observations using transmission electron microscopy (TEM) showed that RCC5270 possesses three types of organic body scales, rather than two as originally described for *P. sorokinii*. We found that the occurrence of three scale types is likely to have been overlooked in the original descriptions of both *P. sorokinii* and *C. birgeri*. We also found that environmental metabarcodes identical to the sequence of RCC5270 were abundant at the location from which *C. birgeri* was initially described (Gulf of Finland). We conclude that *P. sorokinii* and *C. birgeri* are conspecific and *P. sorokinii* is therefore synonymous with *C. birgeri*. Based on its phylogenetic placement and nomenclatural priority, we propose the new combination *Pseudohaptolina birgeri* and emend the description of this species.

ARTICLE HISTORY

Received 19 June 2020

Accepted 25 September 2020

Published online 30 October 2020

KEYWORDS

Arctic phytoplankton;
Chrysochromulina birgeri;
Organic body scale;
Pseudohaptolina

INTRODUCTION

Haptophyte identification is based on both molecular phylogeny and comparison of morphological features such as cell shape, length and movement of the haptonema, and ornamentation of organic body scales. The genus *Pseudohaptolina* was erected from the former *Chrysochromulina* B1-3 clade (Edvardsen *et al.* 2011). Like most haptophytes, *Pseudohaptolina* are solitary, flagellated, and photosynthetic, with two species currently described: the type species *Pseudohaptolina arctica* Edvardsen & Eikrem (Edvardsen *et al.* 2011) and *Pseudohaptolina sorokinii* Stonik, Efimova & Orlova (Orlova *et al.* 2016). *Chrysochromulina birgeri* Hällfors & Niemi (Hällfors & Niemi 1974) was described before the genus *Pseudohaptolina* was erected but is expected to be incorporated within *Pseudohaptolina* based on its morphological similarity to members of this genus. *Pseudohaptolina* species were described from high-latitude Northern Hemisphere marine waters, with *P. arctica* collected from arctic waters in northern Baffin Bay and *P. sorokinii* during an under-ice algal bloom in Amurskiy Bay in the northwestern Sea of Japan (Orlova *et al.* 2016). The type material of *C. birgeri* was collected during an almost unialgal under-ice bloom off the southern coast of Finland (Hällfors & Niemi 1974).

The shape, size, and ornamentation of the organic body scales are taxonomically important characters in Haptophyta, and usually more than one type of body scale occurs per species. The

discrimination between *C. birgeri* and other *Pseudohaptolina* species is possible only through morphological examination, because no molecular data or culture strains are available from its first description (Hällfors & Niemi 1974). *C. birgeri*, *P. arctica*, and *P. sorokinii* were all described as possessing two types of body scales (Hällfors & Thomsen 1979; Edvardsen *et al.* 2011; Orlova *et al.* 2016), usually referred to as ‘small’ and ‘large’ scales.

In the present work, we report morphological and molecular observations along with oceanic distribution for a new strain of *Pseudohaptolina*, which was isolated from Canadian Arctic waters in 2016 (Gérikas Ribeiro *et al.* 2020). This allowed comparison with previously described *Pseudohaptolina* species using morphological and genetic features.

MATERIAL AND METHODS

Strain RCC5270 was isolated into clonal culture from Canadian Arctic waters in 2016 (Gérikas Ribeiro *et al.* 2020), more specifically from Baffin Bay, close to the Inuit village of Qikiqtaurjaq, Nunavut, on Baffin Island (67°28'N, 63°47'W). The strain was identified using 18S rRNA gene sequencing and optical microscopy and deposited in the Roscoff Culture Collection (<http://roscoff-culture-collection.org>) as strain RCC5270. Strain RCC5268 was recovered from the same sample as RCC5270,

and its 18S rRNA sequence (MH764749) shares 100% similarity with that of RCC5270 (MT311519).

Samples for transmission electron microscopy (TEM) were prepared as whole mounts fixed with osmium vapour following Eikrem (1996) with slight modifications (cooling of all equipment). Observations were made using a JEOL JEM-2010 FEG at the Imaging Core Facility at the Station Biologique de Roscoff, France. The sizes of more than 100 scales from RCC5270 and RCC5268 were measured from TEM micrographs using the imaging software ImageJ (Schneider et al. 2012; representative images at <http://www.roscoff-culturecollection.org/rcc-strain-details/5270>).

The nearly complete 18S rRNA gene was amplified using the primers 63F (5'-ACGCTTGTCTCAAAGATTA-3') and 1818R (5'-ACGGAAACCTTGTTACGA-3'; Lepère et al. 2011) and sequenced using the same primers and the internal primer 528F (5'CCGCGGTAATTCCAGCTC-3'; Zhu et al. 2005). The 28S rRNA gene was amplified and sequenced using primers D1R (5'-ACCCGCTGAATTAAAGCATA-3') and D3Ca (5'ACGAACGATTGCACGTCAG-3'; Lenaers et

al. 1989). Sequencing was performed at Macrogen Europe (<https://dna.macrogen-europe.com>). Consensus sequences were generated using de novo assembly in Geneious 10 (Kearse et al. 2012). The RCC5270 18S and 28S rRNA gene sequences were deposited in GenBank under accession numbers MT311519 and MT311520, respectively. For phylogenies, sequences from strain RCC5270 were aligned with closely related Haptophyta sequences from Genbank using the MUSCLE plugin in Geneious 10 (Kearse et al. 2012).

In order to determine the oceanic distribution of the species corresponding to RCC5270, we examined a large set of publicly available metabarcode datasets (Table 1) covering the V4 and V9 regions of the 18S rRNA gene. Twenty-one oceanic 18S rRNA metabarcode datasets were downloaded and reprocessed using the *dada2* R package (Callahan et al. 2016) following the standard operating procedure to produce amplicon single variants (ASVs). The taxonomy of each ASV was assigned using the *dada2* assignTaxonomy function against version 4.12 of the PR² database (Guillou et al. 2013; available at <https://github.com/pr2database/pr2database/>

Table 1. Datasets considered for metabarcode analysis.^a

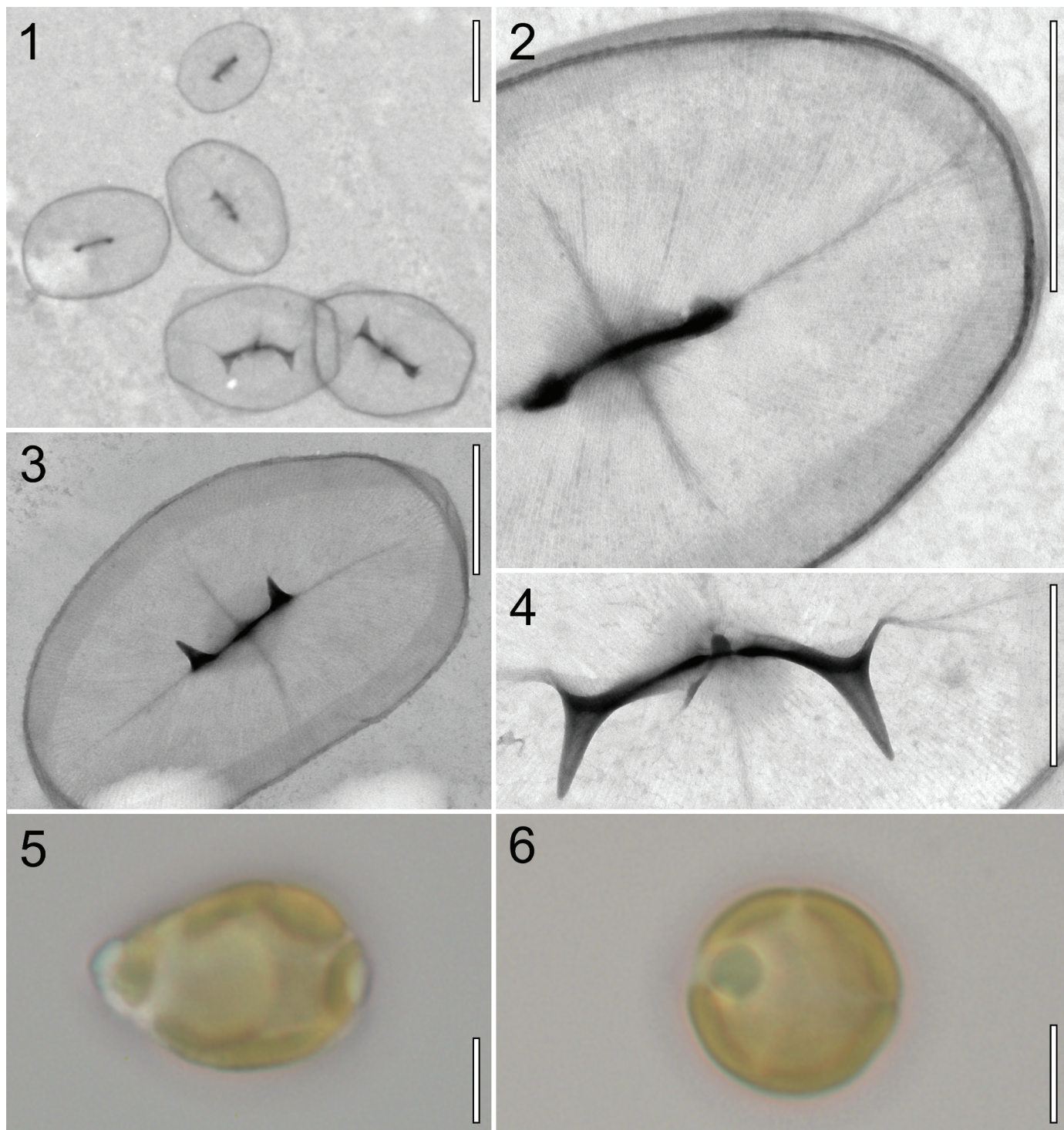
ID	Gene region	Description	Oceanic region	Bioproject or repository	DOI paper	Reads	Substrate
5	V4	Arctic Ocean, Beaufort Sea, MALINA cruise – 2009	Arctic Ocean	PRJNA202104	10.1038/ismej.2014.197		water
6	V4	Central Arctic Ocean – 2012	Arctic Ocean	PRJEB7577	10.1080/09670262.2015.1077395	16	ice
9	V4	Nansen Basin – 2012	Arctic Ocean	PRJEB11449	10.1371/journal.pone.0148512		water
37	V4	Baffin Bay – 2013	Arctic Ocean	PRJNA383398	10.1038/s41598-018-27705-6		water
38	V4	White Sea – 2013–2015	Arctic Ocean	PRJNA368621	10.1007/s00248-017-1076-x	62	ice
39	V4	Arctic Ocean – Polarstern expedition ARK-XXVII/3 – 2012	Arctic Ocean	PRJEB23005	10.3389/fmicb.2018.01035	14,212	water, ice, ice-algal aggregates
40	V4	Arctic Ocean Survey – 2005–2011	Arctic Ocean	PRJNA243055	10.1128/AEM.02737-14	17	water
41	V4	Chukchi Sea – ICESCAPE – 2010	Arctic Ocean	PRJNA217438	10.1128/AEM.02737-14		water
42	V4	Nares Strait – 2014	Arctic Ocean	PRJEB24314	10.3389/fmars.2019.00479	65,898	water
20	V4	Oslo fjord – 2009–2011	Atlantic Ocean	PRJNA497792	10.1111/jeu.12700		water
19	V4	Gulf of Finland – 2012–2013	Baltic Sea	PRJEB21047	10.3354/meps12645	127,118	water, ice
43	V4	Gdansk Gulf – 2012	Baltic Sea	PRJEB23971	10.1002/lno.11177		water
36	V4	Blanes Time Series – 2004–2013	Mediterranean Sea	PRJEB23788	10.1111/mec.14929		water
49	V4	Bay of Naples – 2011	Mediterranean Sea	PRJEB24595	10.1093/femsec/fiw200		water
1	V4	Ocean Sampling Day 2014 V4 LGC	Ocean survey	PRJEB8682	10.1186/s13742-015-0066-5		water
2	V4	Ocean Sampling Day 2015 V4	Ocean survey	https://github.com/MicroB3-IS/osd-analysis/wiki/Guide-to-OSD-2015-data	10.1186/s13742-015-0066-5		water
3	V4	Ocean Sampling Day 2014 V4 LW	Ocean survey	https://github.com/MicroB3-IS/osd-analysis/wiki/Guide-to-OSD-2014-data	10.1186/s13742-015-0066-5		water
34	V4	Malaspina expedition – vertical profiles – 2010–2011	Ocean survey	PRJEB23771	10.1038/s41396-019-0506-9		water
35	V4	Malaspina expedition – surface – 2010–2011	Ocean survey	PRJEB23913			water
11	V4	Fieldes Bay, Antarctic – 2013	Southern Ocean	PRJNA254097	10.1007/s00300-015-1815-8		water
15	V9	Tara Oceans – 2009–2012	Ocean survey	PRJEB6610	10.1126/science.1261605		water

^aThese 21 datasets correspond to the V4 (20) and V9 (1) regions of the 18S rRNA gene. All datasets have been processed with *dada2* software (Callahan et al. 2016) to extract ASVs and assigned using the PR² database (Guillou et al. 2013). ID corresponds to the identification number of the dataset. Reads correspond to the number of sequences in each dataset that could be assigned to RCC5270.

releases/tag/v4.12.0). Twenty datasets corresponded to the V4 of the 18S rRNA gene, and one to the V9 region (Tara Oceans). ASVs with a 100% match to the sequence of RCC5270 were selected and the number of reads in each sample was determined using the R library dplyr. Maps and figures were drawn using the R libraries *ggplot2*, *sf*, and *cowplot*.

RESULTS

In general, the scale morphology of RCC5270 revealed by TEM corresponded closely to those described for *C. birgeri* and *P. sorokinii*, including a radial pattern of ribs arranged in quadrants that coincided with the two orthogonal axes of the scale and two horn-like projections connected by a straight or



Figs 1–6. *Pseudohaptolina*, transmission electron microscope and light microscope images of RCC5270.

Fig. 1. Three types of scales: small (top), medium with short connecting bridges (middle), and large scales (bottom). Scale bar = 1 μm .

Fig. 2. Detail of small scale with approximately 38 ribs in each quadrant. Scale bar = 0.5 μm .

Fig. 3. Medium ellipsoid scale. Scale bar = 1 μm .

Fig. 4. Detail of slightly curved bridge from large scale. Scale bar = 0.5 μm .

Fig. 5. Light microscopy of RCC5270 showing oblong cell. Scale bar = 5 μm .

Fig. 6. Light microscopy of RCC5270 showing round cell with four parietal chloroplasts. Scale bar = 5 μm .

Table 2. Comparison of organic scale measurements between RCC5270, original description of *P. sorokinii* (Orlova et al. 2016), *P. sorokinii* independent measurements from images in Orlova et al. (2016), and *C. birgeri* original description (Hällfors & Niemi 1974).

RCC5270	<i>P. sorokinii</i> description	<i>P. sorokinii</i> images	<i>C. birgeri</i> description	
Scale length (μm)				
Small	1.1–1.4 (1.3 ± 0.1)	1.6–2.0 (1.9 ± 0.03)	1.67–1.73	1.5–1.7
Medium	1.5–2.4 (1.8 ± 0.2)	NA	1.8–2.2	NA
Large	1.9–2.5 (2.2 ± 0.2)	2.1–3.2 (2.6 ± 0.1)	2.7–2.8	2.2–2.6
Scale width (μm)				
Small	0.6–1.0 (0.8 ± 0.1)	1.2–1.9 (1.5 ± 0.05)	0.90–0.95	1.1–1.4
Medium	1.1–1.7 (1.3 ± 0.1)	NA	1.3–2.0	NA
Large	1.1–1.8 (1.5 ± 0.2)	1.6–2.3 (1.9 ± 0.1)	1.5–1.61	1.7–2.1
Distance between horn bases (μm)				
Small	0.2–0.4 (0.3 ± 0.04)	0.3–0.4 (0.40 ± 0.02)	0.34–0.37	0.3–0.4
Medium	0.3–0.6 (0.4 ± 0.1)	NA	0.4–0.5	NA
Large	0.6–1.1 (0.7 ± 0.1)	0.5–0.9 (0.7 ± 0.04)	1.02–1.03	0.4–0.8
Horn measurements (μm)				
Small	0.1–0.2 (0.10 ± 0.04)	0.2–0.4 (0.30 ± 0.02)	0.26–0.30	0.1–0.2
Medium	0.1–0.2 (0.20 ± 0.03)	NA	0.3–0.4	NA
Large	0.2–0.6 (0.3 ± 0.1)	0.5–0.9 (0.70 ± 0.03)	0.7–0.8	0.2–0.6
Number of ribs per quadrant				
Small	37–39	49–57 (52.2 ± 0.80)	NA	c. 38
Medium	54–56	NA	54–60	NA
Large	63–68	52–64 (57.8 ± 1.5)	NA	55–68

slightly curved bridge (Figs 1–6). However, both morphometric data and observations of TEM images of RCC5270 indicated that at least three types of organic scales could be differentiated (Table 2, Figs 1–4) using scale length and width, distance between the horns, and number of radial ribs per quadrant (Figs 7, 8). Small scales of strain RCC5270 had 37–39 ribs per quadrant (Fig. 2), as in the description of *C. birgeri* (Hällfors & Thomsen 1979); whereas, medium scales had 54–56 ribs, and large scales had 63–68 radial ribs per quadrant (Table 2). The distinction between small and medium scales was, however, most readily visible when comparing scale length versus width (Fig. 7). Medium and large scales had somewhat overlapping sizes, so their separation was better achieved by comparing distance between the horn bases versus width (Fig. 8). This was due to a clear distinctive horn bridge structure, with large scales presenting bigger and usually slightly curved bridges (Figs 1–4).

When measurements were conducted on images displayed in the original descriptions, we found that three types of scales could be distinguished for *P. sorokinii* (Figs 7–11) and *C. birgeri* (Figs 12–14). Two types of organic scales of *P. sorokinii*, identified as ‘small scales’ in the original description (Figs 10, 11; see also Orlova et al. 2016, p. 510), fell in the same size range as the ‘medium’ scales identified here (Figs 7, 8). This impacted the number of ribs counted. In addition, independent measurements of small scales depicted in Fig. 8 of the original paper (Fig. 9 in the present work), which were true small scales, fell outside the size range of small scales described by Orlova et al. (2016; Figs 7, 8).

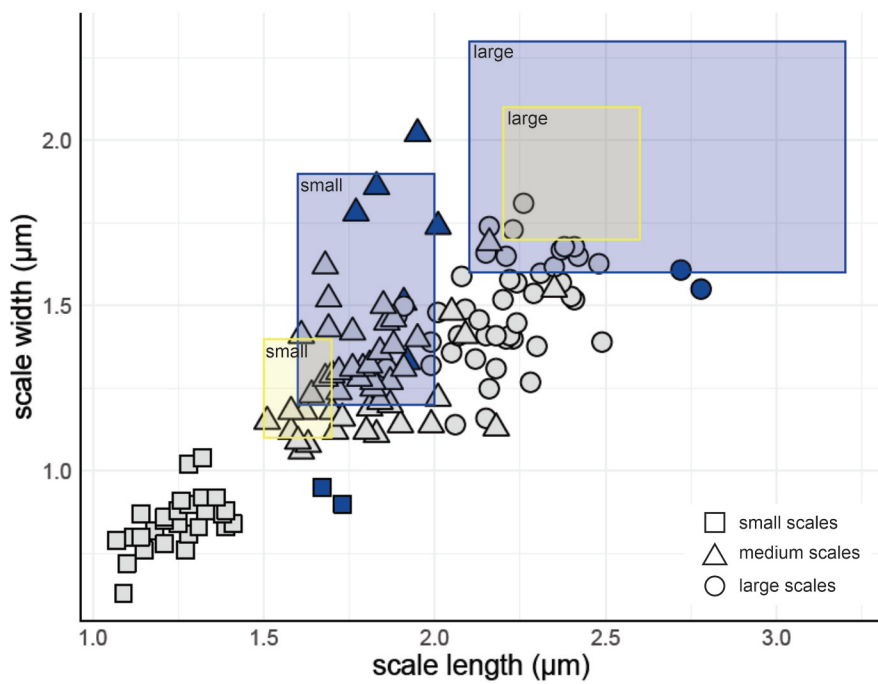
The 18S rRNA gene sequence from RCC5270 was compared with similar sequences including those from previously described *Pseudohaptolina* species. The best match of the sequence was to the two 18S rRNA sequences of *P. sorokinii* in GenBank

(KF684962 and KU589286), both linked to its original description, although only KF684962 is cited in the text of the original description. The 18S rRNA gene sequence of strain RCC5270 differed from sequence KF684962 by five base pairs (four substitutions and one deletion) in a 1655 bp alignment, and by only one base-pair deletion when compared to KU589286 (1213 bp alignment). The divergences from KF684962 seemed to originate from sequencing errors in the description of *P. sorokinii*, because they occurred in well-conserved positions (Fig. 15), and when there was a base variation within these positions in related haptophytes, they did not match those in the *P. sorokinii* sequence (Fig. 15). Furthermore, the two sequences linked to the original description of *P. sorokinii* did not share the same substitutions.

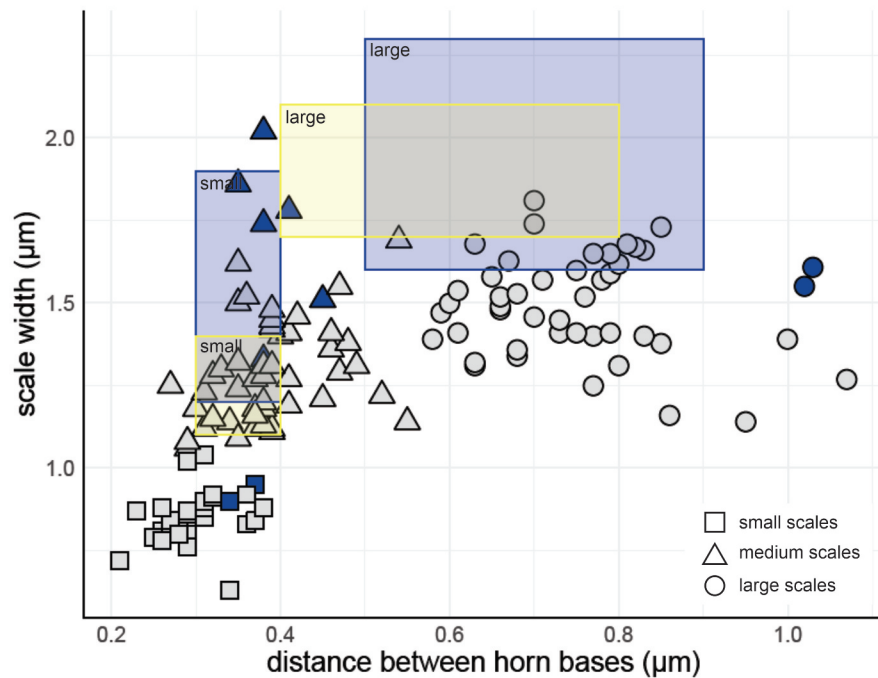
The 28S rRNA gene sequence from RCC5270 had a six base pair difference to the only sequence of *P. sorokinii* 28S rRNA available in GenBank (KU589284), which did not originate from the same isolate used for the description of *P. sorokinii* and is not mentioned in Orlova et al. (2016). The closest hits for both RCC5270 28S rRNA and KU589284 in GenBank corresponded to the environmental clone KU898784 from a sea ice sample in the Barrow Sea (Hassett et al. 2017), with 100% and 98% similarity, respectively.

The metabarcode datasets used to determine the oceanic distribution of RCC5270 corresponded to more than 2200 samples included in large-scale surveys such as Ocean Sampling Day and the Tara Oceans and Malaspina expeditions (de Vargas et al. 2015; Kopf et al. 2015; Logares et al. 2020) that sampled a wide range of coastal and oceanic waters as well as more limited studies of polar waters and the Baltic Sea. We did not retrieve any V9 metabarcodes identical to the RCC5270 sequence. We did, however, retrieve six V4 metabarcodes (ASVs) that were 100% identical to the RCC5270 sequence (Fig. S1). In contrast,

7



8



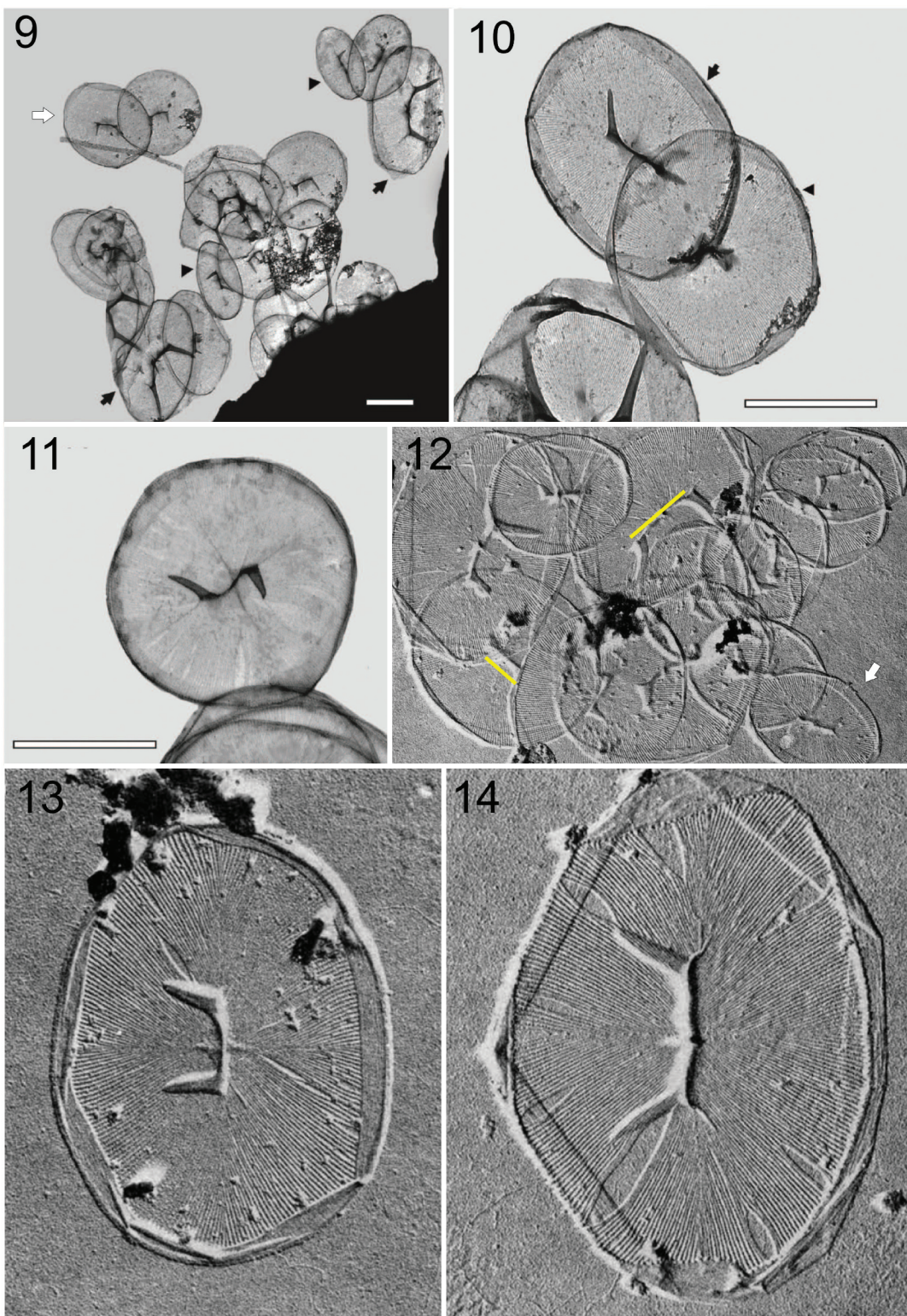
Figs 7, 8. Organic scale measurements of RCC5270 (grey) and independent measurements of *Pseudohaptolina sorokinii* (blue) from images in Orlova *et al.* (2016). Scales visually identified as small are represented by squares, medium scales are represented by triangles, and large scales are represented by circles. Size limits for *C. birgeri* described in Hällfors & Niemi (1974) and size limits for *P. sorokinii* described in Orlova *et al.* (2016) are displayed as yellow and blue boxes, respectively.

Fig. 7. Scale length versus width.

Fig. 8. Scale length versus distance between horns.

no exact match was found for either strain KF684962 or KU589286 of *P. sorokinii* in any of these datasets, which further corroborated the assumption that the mismatches between 18S rRNA *P. sorokinii* and RCC5270 sequences were due to sequencing errors. The RCC5270 metabarcodes were observed only in the Arctic Ocean and in the Baltic Sea from ice and water samples, as well as from algal aggregates collected from the deep-sea floor (Figs 16, 17). Metabarcodes identical to the

sequence of RCC5270 were particularly abundant in three datasets (Table 1) from the *Polarstern* expedition in the Central Arctic Ocean (Rapp *et al.* 2018); from the Nares Strait, the northernmost outflow gateway of Baffin Bay (Kalenitchenko *et al.* 2019); and from the Gulf of Finland (Baltic Sea; Enberg *et al.* 2018). At the latter location, which corresponded to the region from which *C. birgeri* was initially described, metabarcodes identical to the RCC5270 sequence first appeared in February



Figs 9–14. TEM of *Pseudohaptolina sorokinii* and *Chryschromulina birgeri* modified from Orlova et al. (2016) and Hälfors & Thomsen (1979), respectively. Scale bar = 1 μm for *P. sorokinii*; no scale bar was available for *C. birgeri*.

Fig. 9. Organic body scales of *P. sorokinii* showing three types: small (arrow heads), large (arrows), and medium (white arrow, not mentioned in the description paper).

Fig. 10. Scales of *P. sorokinii* identified as small by Orlova et al. (2016), although measurements fall within the medium scale size range because they are noticeably larger than the small scales identified in previous image.

Fig. 11. Scale of *P. sorokinii* identified as small in the description paper; its round structure, length, and width are similar to medium scales.

Fig. 12. Scale of *C. birgeri* with yellow lines highlighting differences in connecting bridge between horn bases, the main feature used to distinguish large from medium scales in the present study. For size comparison, one small scale can be seen in the lower right corner of the image (white arrow).

Fig. 13. Scale of *C. birgeri*, identified as large by Hälfors & Thomsen (1979), although its features, including number of ribs per quadrant (54), correspond to a medium size scale.

Fig. 14. True large scale of *C. birgeri*, with longer distance between horn bases and a slightly curved bridge.

		790	800	810
1. KF684962 - <i>Pseudohaptolina sorokinii</i>	A A A T A G G A C T T T G	T	T	T G G T T T C G A A C
2. KU589286 - <i>Pseudohaptolina sorokinii</i>	A A A T A G G A C T T T G	G T G C T A T T T T G T T G G T T T C G A A C		
3. MT311519 - <i>Pseudohaptolina</i> sp.	A A A T A G G A C T T T G	G T G C T A T T T T G T T G G T T T C G A A C		
4. AF163147 - <i>Phaeocystis cordata</i>	A A A T A G G A C T C T G	C T G G T G C T A T T T T G T T G G T T T C G A A C		
5. AF163148 - <i>Phaeocystis jahnnii</i>	A A A T A G G A C T C T G	C T G G T G C T A T T T T G T T G G T T T C G A A C		
6. AJ246264 - <i>Pleurochrysis elongata</i>	A A A T A G G A C T C T G	C T G G T G C T A T T T T G T T G G T T T C G A A C		
7. AJ544120 - <i>Chrysotila carterae</i>	A A A T A G G A C T C T G	C T G G T G C T A T T T T G T T G G T T T C G A A C		
8. AJ544121 - <i>Pleurochrysis dentata</i>	A A A T A G G A C T C T G	C T G G T G C T A T T T T G T T G G T T T C G A A C		
9. AM491017 - <i>Chrysochromulina leadbeateri</i>	A A A T A G G A C T T T G	G T G C T A T T T T G T T G G T T T C G A A C		
10. AF107080 - unidentified prymnesiophyte clone OLI16029	A A A T A G G A C T T T G	G T G C T A T T T T G T T G G T T T C G A A C		
11. AM491021 - <i>Chrysochromulina simplex</i>	A A A T A G G A C T T T G	G T G C T A T T T T G T T G G T T T C G A A C		
12. AJ246274 - <i>Chrysochromulina scutellum</i>	A A A T A G G A C T T T G	G T G C T A T T T T G T T G G T T T C G A A C		
13. AM491018 - <i>Chrysochromulina cymbium</i>	A A A T A G G A C T T T G	G T G C T A T T T T G T T G G T T T C G A A C		
14. AJ246273 - <i>Chrysochromulina campanulifera</i>	A A A T A G G A C T T T G	G T G C T A T T T T G T T G G T T T C G A A C		
15. FN599060 - <i>Chrysochromulina strobilus</i>	A A A T A G G A C T T T G	G T G C T A T T T T G T T G G T T T C G A A C		
16. AM491019 - <i>Chrysochromulina parva</i>	A A A T A G G A C T T T G	G T G C T A T T T T G T T G G T T T C G A A C		
17. AJ246277 - <i>Chrysochromulina throndsenii</i>	A A A T A G G A C T T T G	G T G C T A T T T T G T T G G T T T C G A A C		
18. FN599059 - <i>Chrysochromulina acantha</i>	A A A T A G G A C T T T G	G T G C T A T T T T G T T G G T T T C G A A C		
19. AB199882 - <i>Chrysochromulina</i> sp. MBIC10513	A A A T A G G A C T T T G	G T G C T A T T T T G T T G G T T T C G A A C		
20. AM491025 - <i>Chrysochromulina rotalis</i>	A A A T A G G A C T T T G	G T G C T A T T T T G T T G G T T T C G A A C		
21. AJ246266 - <i>Isochrysis galbana</i>	A A A T A G G A C T C T G	C T G G T G C T A T T T T G T T G G T T T C G A G		
22. AJ246276 - <i>Gephyrocapsa oceanica</i>	A A A T A G G A C T C T G	C T G G T G C T A T T T T G T T G G T T T C G A A C		
23. AJ246262 - <i>Cruciplacolithus neohelis</i>	A A A T A G G A C T C T G	C T G G T G C T A T T T T G T T G G T T T C G A A C		
24. AJ544117 - <i>Coccothithus braarudii</i>	A A A T A G G A C T C T G	C T G G T G C T A T T T T G T T G G T T T C G A A C		
25. AM491022 - <i>Chrysocampanula spinifera</i>	A A A T A G G A C T T T G	G T G C T A T T T T G T T G G T T T C G A A C		
26. AB183265 - <i>Prymnesium neolepis</i>	A A A T A G G A C T T T G	G T G C T A T T T T G T T G G T T T C G A G		
27. AJ246267 - <i>Imantonia rotunda</i>	A A A T A G G A C T C T G	C T G G T G C T A T T T T G T T G G T T T C G A G		
28. AM491015 - cf. <i>Imantonia</i> sp. CCMP1404	A A A T A G G A C T C T G	C T G G T G C T A T T T T G T T G G T T T C G A G		
29. AM491016 - <i>Pseudohaptolina arctica</i>	A A A T A G G A C T T T G	G T G C T A T T T T G T T G G T T T C G A A C		
30. AB058358 - <i>Haptolina brevifila</i>	A A A T A G G A C T T T G	G T G C T A T T T T G T T G G T T T C G A A C		
31. AM491010 - <i>Prymnesium minus</i>	A A A T A G G A C T T T G	G T G C T A T T T T G T T G G T T T C G A A C		
32. AM491011 - <i>Haptolina</i> cf. <i>herdlensis</i>	A A A T A G G A C T T T G	G T G C T A T T T T G T T G G T T T C G A A C		
33. AJ246272 - <i>Haptolina hirta</i>	A A A T A G G A C T T T G	G T G C T A T T T T G T T G G T T T C G A A C		
34. AM491030 - <i>Haptolina ericina</i>	A A A T A G G A C T T T G	G T G C T A T T T T G T T G G T T T C G A A C		
35. AM491012 - <i>Haptolina brevifila</i>	A A A T A G G A C T T T G	G T G C T A T T T T G T T G G T T T C G A A C		
36. AM491013 - <i>Haptolina fragaria</i>	A A A T A G G A C T T T G	G T G C T A T T T T G T T G G T T T C G A A C		
37. AM491003 - <i>Prymnesium pigrum</i>	A A A T A G G A C T T T G	G T G C T A T T T T G T T G G T T T C G A A C		
38. AJ246268 - <i>Prymnesium nemamethicum</i>	A A A T A G G A C T T T G	G T G C T A T T T T G T T G G T T T C G A A C		
39. AJ246271 - <i>Prymnesium kappa</i>	A A A T A G G A C T T T G	G T G C T A T T T T G T T G G T T T C G A A C		
40. AM491029 - <i>Prymnesium chiton</i>	A A A T A G G A C T T T G	G T G C T A T T T T G T T G G T T T C G A A C		
41. AJ004866 - <i>Prymnesium polylepis</i>	A A A T A G G A C T T T G	G T G C T A T T T T G T T G G T T T C G A A C		
42. AJ004868 - <i>Prymnesium</i> aff. <i>polylepis</i>	A A A T A G G A C T T T G	G T G C T A T T T T G T T G G T T T C G A A C		
43. AM491001 - <i>Prymnesium</i> sp. ALGO HAP pt	A A A T A G G A C T T T G	G T G C T A T T T T G T T G G T T T C G A A C		
44. AM491001 - <i>Prymnesium zebrinum</i>	A A A T A G G A C T T T G	G T G C T A T T T T G T T G G T T T C G A A C		
45. AM491027 - <i>Prymnesium pienaarii</i>	A A A T A G G A C T T T G	G T G C T A T T T T G T T G G T T T C G A A C		
46. AM491028 - <i>Prymnesium simplex</i>	A A A T A G G A C T T T G	G T G C T A T T T T G T T G G T T T C G A A C		
47. AM491008 - <i>Prymnesium calathiferum</i>	A A A T A G G A C T T T G	G T G C T A T T T T G T T G G T T T C G A A C		
48. AM491005 - <i>Prymnesium faveolatum</i>	A A A T A G G A C T T T G	G T G C T A T T T T G T T G G T T T C G A A C		
49. AM491007 - <i>Prymnesium annuliferum</i>	A A A T A G G A C T T T G	G T G C T A T T T T G T T G G T T T C G A A C		

Fig. 15. Partial V4 18S rRNA gene sequence alignment showing RCC5270 (MT311519) and *Pseudohaptolina sorokinii* KF684962 sequence in comparison to closely related groups; three substitutions are visible in the latter, but they are not shared by any other sequence, including *P. sorokinii* KU589286.

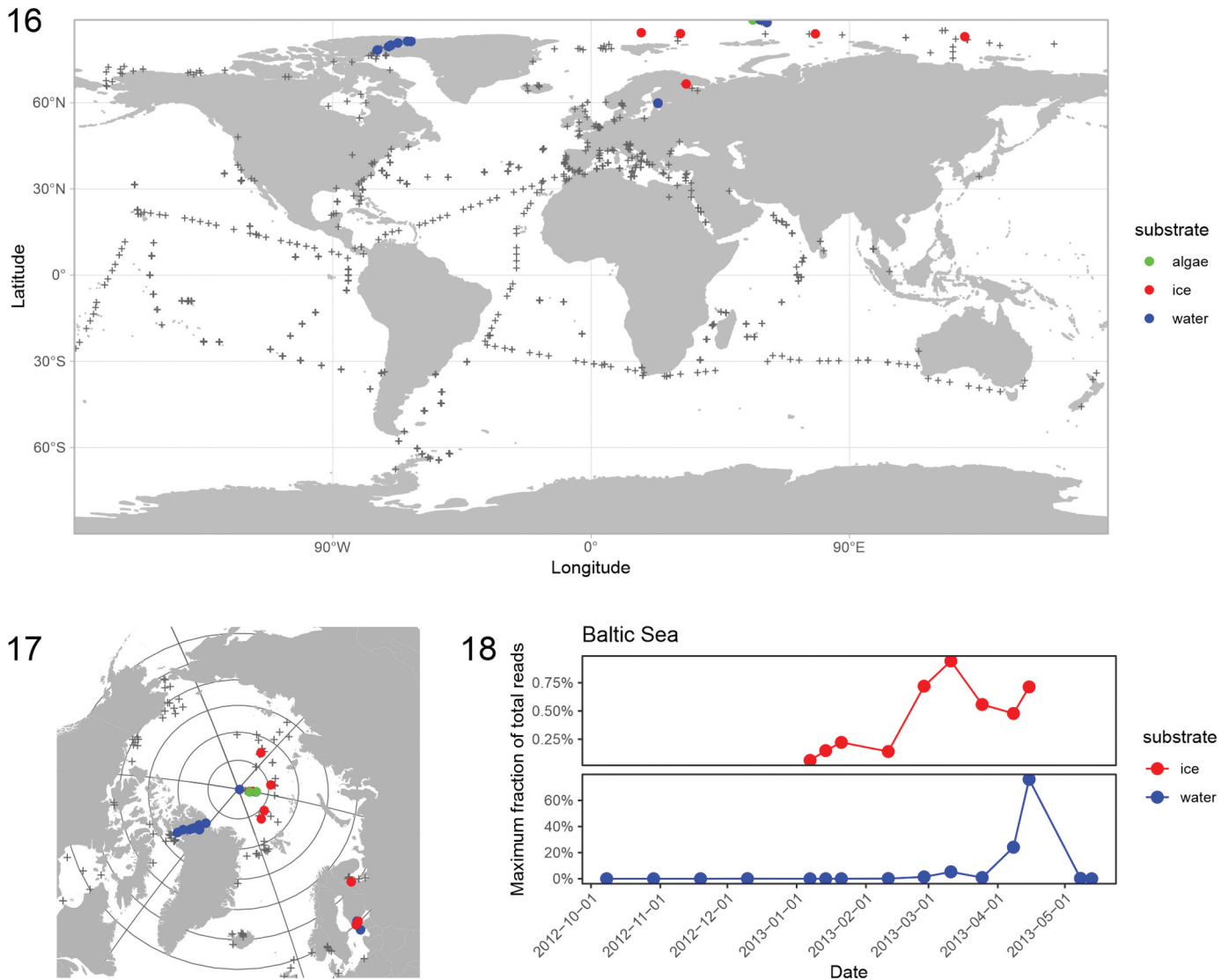
in the ice, where they peaked in early March, and then increased massively in the water column one month later, representing up to 70% of the metabarcodes when the ice melted in mid-April (Fig. 18).

DISCUSSION

From the description of *P. sorokinii* (Orlova *et al.* 2016), three morphological features of the organic body scales are considered sufficiently distinct from *C. birgeri* to assign *P. sorokinii* as a new species; these features are horn morphology, shape of the connecting bridge, and density of radial ribs. However, apart from the feature ‘number of radial ribs arranged in quadrants’ present in the so-called small scales, all other measurements overlap to some extent with those recorded for *C. birgeri* (see table 1 in Orlova *et al.* 2016, p. 511). The identification of a third organic body scale type, which has been overlooked in descriptions of both *P. sorokinii* and *C. birgeri*, indicates that rib counts in those studies might be inaccurate. Unfortunately, the resolution of available images of *P. sorokinii* is insufficient to perform an independent count of the ribs in the small scales. The size of the connecting

bridge was used by Orlova *et al.* (2016) as a distinctive feature of large scales. Thus, small and medium scales were probably grouped together, which might have led to the discrepancies observed in the number of ribs per quadrant reported in the description of *P. sorokinii*. In contrast, in the description of *C. birgeri*, medium and large scales with evident differences in the connecting bridge structure were grouped together as ‘large’ (Figs 13, 14). It is noteworthy that scale measurements of neither *P. sorokinii* nor RCC5270 corresponded precisely to the size limits described for *C. birgeri* (Hällfors & Thomsen 1979), particularly for small scales (Figs 7, 8).

Other morphological characters used to differentiate *P. sorokinii* from *C. birgeri* by Orlova *et al.* (2016) are horn length and the shape of the connecting bridge. Orlova *et al.* (2016) reported long horn projections and curved connecting bridges, in contrast to the description of *C. birgeri*, although long horn-like projections connected by a curved bridge in large scales have already been reported for *C. birgeri* (Hällfors & Thomsen 1979; Takahashi 1981). The horn projections of large scales of RCC5270 are in general smaller than those observed by Orlova *et al.* (2016) but are somewhat superimposed within their size range (Table 2). We also observed



Figs 16–18. Metabarcodes of RCC5270.

Fig. 16. Location of stations where 18S rRNA metabarcodes 100% identical to RCC5270 sequence have been detected in public sequence datasets (see Table 1). Colour corresponds to substratum. Location of samples where these metabarcodes have not been detected are marked by grey crosses.

Fig. 17. North Pole visualisation of stations where 18S rRNA metabarcodes were 100% identical to RCC5270 sequence.

Fig. 18. Maximum fraction of metabarcodes of RCC5270 (excluding Metazoa) as a function of date in the Gulf of Finland (Baltic Sea) in ice and water (Enberg et al. 2018).

curved connecting bridges in the large scales (Fig. 1). Thus, there is considerable overlap but some variability in the size and features of scales of RCC5270, *P. sorokinii*, and *C. birgeri*, which might reflect morphological plasticity within a single species because heteromorphic life cycles have been observed within the Prymnesiales (Paasche et al. 1990; Edvardsen & Vaulot 1996).

The 18S rRNA gene metabarcode survey indicates that RCC5270 is an ice alga with pan-Arctic distribution, which can seed and proliferate in the water column, and even accumulate on the deep-sea floor. The lack of an exact match of the 18S rRNA gene sequence for *P. sorokinii* to any of the datasets analysed, along with its divergences from closely related Haptophyta on well conserved positions, corroborates

the assumption that those divergences might have originated from sequencing errors.

CONCLUSIONS

We isolated a culture strain from the Arctic that was genetically affiliated to *P. sorokinii*. Morphological data indicate that a third scale type was overlooked in the original description of *P. sorokinii* (Orlova et al. 2016), impacting the number of radiating ribs described for each scale type. We also found that cells of *C. birgeri* have three types of organic body scale, not two as reported in the original description (Hällfors & Thomsen 1979). Metabarcode data indicate that sequences identical to those of RCC5270 were abundant near the type

locality of *C. birgeri*. We conclude that *P. sorokinii* is conspecific with the formerly described *C. birgeri*. We therefore transfer *C. birgeri* to the genus *Pseudohaptolina* and emend its description. *P. birgeri* is the correct name for this species due to nomenclatural priority over *P. sorokinii*.

ACKNOWLEDGEMENTS

We are grateful to Sophie Le Panse from the Merimage microscopy platform at the Roscoff Marine Station for assistance with the transmission electron micrographs and to the Roscoff Culture Collection for maintenance of the algal strain.

FUNDING

This work was supported by the GreenEdge project (Fondation Total & ANR, under Grant ANR-14-CE01-0017); the ANR PhytoPol under Grant ANR-15-CE02-0007; and TaxMArc (Research Council of Norway, under Grant 268286/E40). ALS was supported by the Singapore Ministry of Education, Academic Research Fund Tier 1 (RG26/19). CGR was supported by the FONDECYT project number 3190827.

DATA ACCESSIBILITY STATEMENT

Supporting data have been deposited to GitHub: <https://github.com/vaulot/Paper-2020-Ribeiro-Pseudohaptolina>.

ORCID

Catherine Gérikas Ribeiro  <http://orcid.org/0000-0003-0531-2313>
 Adriana Lopes dos Santos  <http://orcid.org/0000-0002-0736-4937>
 Ian Probert  <http://orcid.org/0000-0002-1643-1759>
 Daniel Vaulot  <http://orcid.org/0000-0002-0717-5685>
 Bente Edvardsen  <http://orcid.org/0000-0002-6806-4807>

REFERENCES

- Callahan B.J., McMurdie P.J., Rosen M.J., Han A.W., Johnson A.J.A. & Holmes S.P. 2016. DADA2: high-resolution sample inference from Illumina amplicon data. *Nature Methods* 13: 581–583. DOI: [10.1038/nmeth.3869](https://doi.org/10.1038/nmeth.3869).
- de Vargas C., Audic S., Henry N., Decelle J., Mahe F., Logares R., Lara E., Berney C., Le Bescot N., Probert I. et al. 2015. Eukaryotic plankton diversity in the sunlit ocean. *Science* 348: 1261605. DOI: [10.1126/science.1261605](https://doi.org/10.1126/science.1261605).
- Edvardsen B., Eikrem W., Thronsen J., Sáez A.G., Probert I. & Medlin L.K. 2011. Ribosomal DNA phylogenies and a morphological revision provide the basis for a revised taxonomy of the Prymnesiales (Haptophyta). *European Journal of Phycology* 46: 202–228. DOI: [10.1080/09670262.2011.594095](https://doi.org/10.1080/09670262.2011.594095).
- Edvardsen B. & Vaulot D. 1996. Ploidy analysis of the two motile forms of *Chryschromulina polylepis* (Prymnesiophyceae). *Journal of Phycology* 32: 94–102.
- Eikrem W. 1996. *Chryschromulina thronsenii* sp. nov. (Prymnesiophyceae). Description of a new haptophyte flagellate from Norwegian waters. *Phycologia* 35: 377–380. DOI: [10.2216/0031-8884-35-5-377.1](https://doi.org/10.2216/0031-8884-35-5-377.1).
- Enberg S., Majaneva M., Autio R., Blomster J. & Rintala J.M. 2018. Phases of microalgal succession in sea ice and the water column in the Baltic Sea from autumn to spring. *Marine Ecology Progress Series* 599: 19–34. DOI: [10.3354/meps12645](https://doi.org/10.3354/meps12645).
- Gérikas Ribeiro C., Lopes Dos Santos A., Marie D., Le Gall F., Probert I., Tragin M., Gourvil P. & Vaulot D. 2020. Culturable diversity of Arctic phytoplankton during pack ice melting. *Elementa: Science of the Anthropocene* 8: 6. DOI: [10.1525/elementa.401](https://doi.org/10.1525/elementa.401).
- Guillou L., Bachar D., Audic S., Bass D., Berney C., Bittner L., Boutte C., Burgaud G., de Vargas C., Decelle J. et al. 2013. The Protist Ribosomal Reference Database (PR²): a catalog of unicellular eukaryote small sub-unit rRNA sequences with curated taxonomy. *Nucleic Acids Research* 41: D597–D604. DOI: [10.1093/nar/gks1160](https://doi.org/10.1093/nar/gks1160).
- Hällfors G. & Niemi A. 1974. *Chryschromulina* (Haptophyceae) bloom under the ice in the Tvarminne Archipelago, southern coast of Finland. *Memoranda Societatis pro Fauna et Flora Fennica* 50: 89–104.
- Hällfors G. & Thomsen H.A. 1979. Further observations on *Chryschromulina birgeri* (Prymnesiophyceae) from the Tvarminne Archipelago, SW coast of Finland. *Acta Bot Fennica* 110: 41–46.
- Hassett B.T., Ducluzeau A.L.L., Collins R.E. & Gradinger R. 2017. Spatial distribution of aquatic marine fungi across the western Arctic and sub-Arctic. *Environmental Microbiology* 19: 475–484. DOI: [10.1111/1462-2920.13371](https://doi.org/10.1111/1462-2920.13371).
- Kalenitchenko D., Joli N., Potvin M., Tremblay J.-É. & Lovejoy C. 2019. Biodiversity and species change in the Arctic Ocean: a view through the lens of Nares Strait. *Frontiers in Marine Science* 6: 1–17. DOI: [10.3389/fmars.2019.00479](https://doi.org/10.3389/fmars.2019.00479).
- Kearse M., Moir R., Wilson A., Stones-Havas S., Cheung M., Sturrock S., Buxton S., Cooper A., Markowitz S., Duran C. et al. 2012. Geneious basic: an integrated and extendable desktop software platform for the organization and analysis of sequence data. *Bioinformatics* 28: 1647–1649. DOI: [10.1093/bioinformatics/bts199](https://doi.org/10.1093/bioinformatics/bts199).
- Kopf A., Bicak M., Kottmann R., Schnetzer J., Kostadinov I., Lehmann K., Fernandez-Guerra A., Jeanthon C., Rahav E., Ullrich M. et al. 2015. The ocean sampling day consortium. *GigaScience* 4: 27. DOI: [10.1186/s13742-015-0066-5](https://doi.org/10.1186/s13742-015-0066-5).
- Lenaers G., Maroteaux L., Michot B. & Herzog M. 1989. Dinoflagellates in evolution. A molecular phylogenetic analysis of large subunit ribosomal RNA. *Journal of Molecular Evolution* 29: 40–51. DOI: [10.1007/BF02106180](https://doi.org/10.1007/BF02106180).
- Lepèze C., Demura M., Kawachi M., Romac S., Probert I. & Vaulot D. 2011. Whole-genome amplification (WGA) of marine photosynthetic eukaryote populations. *FEMS Microbiology Ecology* 76: 513–523. DOI: [10.1111/j.1574-6941.2011.01072.x](https://doi.org/10.1111/j.1574-6941.2011.01072.x).
- Logares R., Deutschmann I.M., Junger P.C., Giner C.R., Krabberød A.K., Schmidt T.S.B., Rubinat-Ripoll L., Mestre M., Salazar G., Ruiz-González C. et al. 2020. Disentangling the mechanisms shaping the surface ocean microbiota. *Microbiome* 8: 55. DOI: [10.1186/s40168-020-00827-8](https://doi.org/10.1186/s40168-020-00827-8).
- Orlova T.Y., Efimova K.V. & Stonik I.V. 2016. Morphology and molecular phylogeny of *Pseudohaptolina sorokinii* sp. nov. (Prymnesiales, Haptophyta) from the Sea of Japan, Russia. *Phycologia* 55: 506–514. DOI: [10.2216/15-107.1](https://doi.org/10.2216/15-107.1).
- Paasche E., Edvardsen B. & Eikrem W. 1990. A possible alternate stage in the life cycle of *Chryschromulina polylepis* Manton et Parke (Prymnesiophyceae). *Nova Hedwigia Beiheft* 100: 91–99.
- Rapp J.Z., Fernández-Méndez M., Bienhold C. & Boetius A. 2018. Effects of ice-algal aggregate export on the connectivity of bacterial communities in the central Arctic Ocean. *Frontiers in Microbiology* 9: 1035. DOI: [10.3389/fmicb.2018.01035](https://doi.org/10.3389/fmicb.2018.01035).
- Schneider, C. A.; Rasband, W. S. & Eliceiri, K. W. 2012. NIH Image to ImageJ: 25 years of image analysis. *Nature Methods* 9(7): 671–675. PMID 22930834. <https://imagej.nih.gov/ij/>.
- Takahashi E. 1981. Floristic study of ice algae in the sea ice of a lagoon, Lake Saroma Hokkaido, Japan. *Memoirs of the National Institute of Polar Research* 34: 49–56.
- Zhu F., Massana R., Not F., Marie D. & Vaulot D. 2005. Mapping of picoeucaryotes in marine ecosystems with quantitative PCR of the 18S rRNA

gene. *FEMS Microbiology Ecology* 52: 79–92. DOI: [10.1016/j.femsec.2004.10.006](https://doi.org/10.1016/j.femsec.2004.10.006).

SYNONYM: *Pseudohaptolina sorokinii* Stonik, Efimova & Orlova.

TAXONOMIC APPENDIX

Pseudohaptolina birgeri (Hällfors & Niemi) Ribeiro & Edvardsen comb. nov. emend. Ribeiro & Edvardsen

Basionym *Chrysochromulina birgeri* Hällfors & Niemi in Hällfors & Niemi (1974). Memoranda Societatis pro Fauna et Flora Fennica 50, p. 90. Drawing fig. 4.

EMENDED DESCRIPTION: Scaly covering composed of three round to oval scale types. Small scales have width \times length c. $0.6\text{--}1.4 \times 1.1\text{--}1.7$, medium scales c. $1.1\text{--}2 \times 1.5\text{--}2.4$, and large scales c. $1.1\text{--}2.1 \times 1.9\text{--}2.8$ nm. All scales with radial ribs on both distal and proximal faces. Small scales have 37–39 radial ribs per quadrant, medium scales have 54–60, and large scales have 63–68. Medium and large scales have two horns on the distal face. The distance between horns, and form of the horns, are different in medium and large scales.